

RESEARCH

Open Access



Microstructure Change of Nanosilica–Cement Composites Partially Exposed to Sulfate Attack

Qian Huang¹ , Liang Zhao^{1*}, Chenggong Zhao¹, Dongsheng Liu² and Chaoqiang Wang³

Abstract

The deterioration of cement composites containing nanosilica partially exposed to sulfate attack was studied, and the microstructure change of the composites was analysed by a scanning electron microscope (SEM), energy dispersive spectroscopy (EDS) and X-ray diffraction (XRD). The results showed that nanosilica–cement composites had better sulfate resistance compared to plain cement composite under partial exposure to sulfate attack, and their sulfate resistance increased as the nanosilica content increased (in the range of 0 to 5 wt% replacing cement by weight). The main sulfate products were gypsum and ettringite within the surface and inner parts, respectively in both the immersed and evaporation portions of the nanosilica–cement composites, which was consistent with the plain cement composite. Thus, the incorporation of nanosilica did not change the distribution characteristics of the sulfate products within the composites partially exposed to sulfate attack. However, the addition of nanosilica reduced the amount of sulfate products in both the immersed and evaporation portions, and their amount decreased with the increase of nanosilica content. The evaporation portions of the composites suffered chemical sulfate attack rather than sulfate salt crystallization. Nanosilica–cement composites could be applied in real partial exposure environments containing sulfate ions.

Keywords: nanosilica, cement composites, partial exposure, sulfate attack, microstructure

1 Introduction

In recent years, the performance requirements for cement composites have become increasingly high with societal development, and the modification technology of additives (e.g. supplemental cementitious materials, polymer and nanomaterials) has been studied and applied in cement composites. The addition of supplemental cementitious materials such as fly ash, slag and silica fume could improve the mechanical properties and durability of cement-based materials (Cho et al. 2019; Liu et al. 2019; Olsson et al. 2018). The incorporation of polymers enhanced the chemical stability of cement composites in the environment containing radioactive waste (Eskander et al. 2012; Saleh and Eskander

2019). The use of nanomaterials (e.g. nanofibers, graphene oxide and nanoparticles) could significantly increase their mechanical properties owing to the reduction in porosity of cement-based materials (Saleh et al. 2018, 2019a, b, c; Ghazi-zadeh et al. 2018). Nanosilica, which was one of the earliest nanomaterials applied in cement-based composites, had a more obvious effect on the performance improvement compared to other nanoparticles. This was because nanosilica had high pozzolanic activity and could react with $\text{Ca}(\text{OH})_2$ in cement composites to generate more calcium silicate hydrate (C–S–H gel), thereby making the composites more compact (Said et al. 2012; Yu et al. 2014; Sharma et al. 2019). At present, a great deal of work has been done on the properties of nanosilica–cement composites, such as hydration, early rheological and mechanical properties, durability and microstructure. The incorporation of nanosilica accelerated cement hydration process and effectively improved early strength and durability of cement composites (Jo et al. 2007). However,

*Correspondence: zhaoliang@yznu.edu.cn

¹ School of Civil and Architectural Engineering, Yangtze Normal University, Chongqing 408100, People's Republic of China

Full list of author information is available at the end of the article

Journal information: ISSN 1976-0485 / eISSN 2234-1315

a high amount of nanosilica could not be well-dispersed through the mixture due to agglomeration and consequently, could not effectively exert their function and provide the best results (Stefanidou and Papayianni 2012).

In terms of durability, Jalal et al. (2015) found that incorporating 2% nanosilica decreased capillary water absorption by 58% compared to the control composites without nanosilica. Tobón et al. (2015) also obtained similar results and attributed them to the pozzolanic reaction progress of nanosilica, which reduced the total pore volume and hindered pore connectivity, thereby inhibiting water permeability. Other research results (Atewi et al. 2019; Du et al. 2014; Mohseni et al. 2015) showed that the addition of nanosilica enhanced chloride penetration resistance of concrete composites, because nanosilica refined the pore structure and improved the interfacial transition zone (ITZ). Behfarnia and Salemi (2013) indicated that the frost resistance of concrete containing nanosilica was considerably improved, owing to a more compact microstructure. Atahan and Dikme (2011) investigated the effect of mineral admixtures such as nanosilica, micro silica, fly ash and ground granulated blast furnace slag on the expansion of cement composites caused by a full-immersion sulfate attack, and observed that nanosilica was most effective for limiting expansion. It should be pointed out that the performance change of cement composites under the full-immersion sulfate attack was different from that under the partial-immersion attack. In the partial exposure condition, cement composites were not only affected by sulfate chemical attack, but also damaged by physical salt crystallization.

However, there are few reports on the durability of cement–nanosilica composites partially exposed to sulfate attacks. Therefore, cement composites with nanosilica were partially immersed in a sulfate solution in this study; the damage characteristic of the composites was then investigated, and the composites' microstructure changes were analysed by SEM, EDS and XRD to explore the damage mechanism.

2 Experimental Programs

2.1 Materials and Mix Proportions

P.O 42.5 ordinary Portland cement with a specific gravity of 3.12 g/cm³ was used in this study; its chemical composition is given in Table 1. Fine aggregate with a specific gravity of 2.65 g/cm³ and a fineness modulus of 2.70 was used. The average particle size of colloidal nanosilica was 10 nm (Fig. 1), the specific surface area was 954.3 m²/g, and the SiO₂ purity was more than 99.9%.

In all the cement composites, the ratio of the cementitious materials (including cement and nanosilica) to fine aggregate to water was kept constant at 1:3:0.45 by weight. Nanosilica was added at 0, 1, 3, and 5 wt% of the unit cement mass, and the corresponding numbers of the nanosilica–cement composites were marked as NC0, NC1, NC3 and NC5, respectively.

2.2 Partial Exposure Test

The mixtures were cast in cuboid moulds of 40 mm × 40 mm × 160 mm. The specimens were demoulded after being placed in a lab for 24 h, and then cured for 28 days in a condition of 20 ± 2 °C and above 95% of relative humidity (RH). After curing, the cement composites were dried in a laboratory (at 20 ± 2 °C and 60 ± 5% RH) for 48 h, and then partially immersed in containers with 5% Na₂SO₄ solution and water (as reference group) respectively up to 60 mm. The composites were kept for 12 months in a room condition with 20 °C and 60% RH.

2.3 Test Methods

During the experiment, the appearance damage characteristic of nanosilica–cement composites was visually observed and recorded by taking pictures.

The length of the composites was regularly monitored using a digital calliper with an accuracy of 0.01 mm. Consequently, the linear expansion (LE_n) of the composites was calculated as follows:

$$LE_n = (l_n - l_0)/l_0 \quad (1)$$

where l_0 and l_n are the lengths of the composites before and after the sulfate attack test, respectively.

The compressive strength loss (F_n) of the composites was calculated according to Eq. (2):

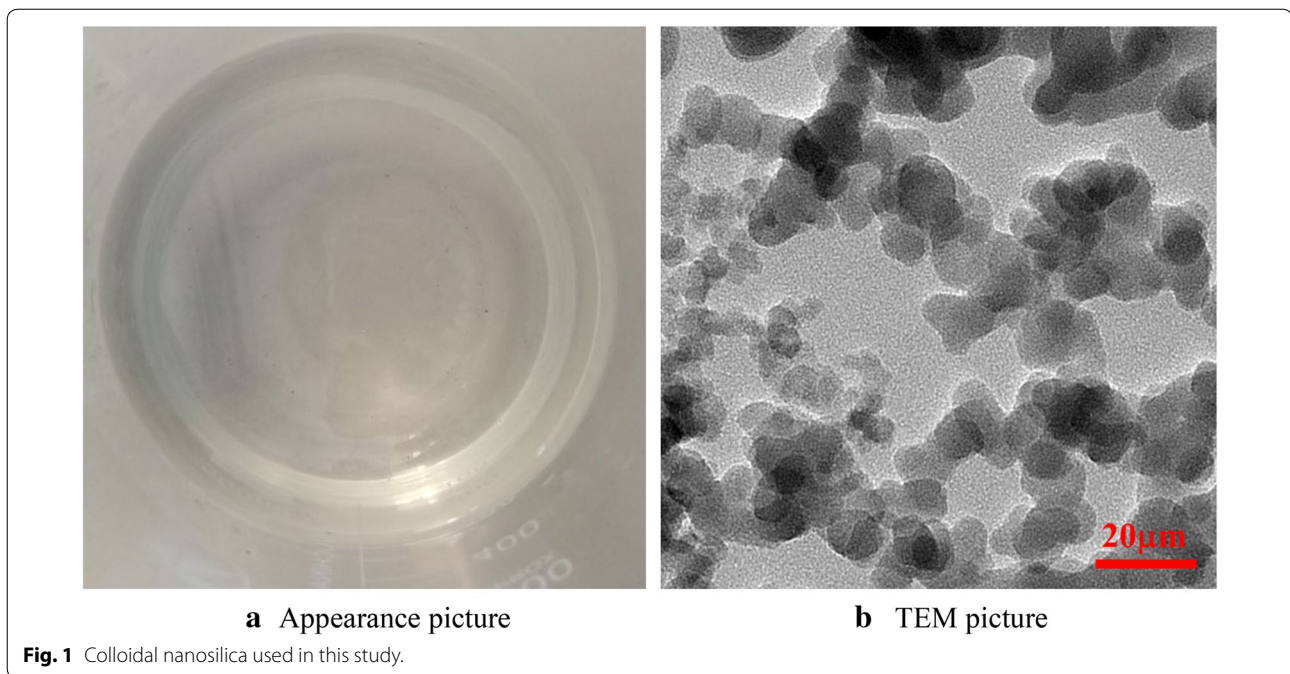
$$F_n = (f_0 - f_n)/f_0 \times 100\% \quad (2)$$

where f_n represents the compressive strength of the immersed and evaporation portions of the composites partially exposed to sulfate attack; f_0 is the corresponding strength of the composites partially exposed to water at the same period. All the above tests were carried out on three samples and the given results are average values.

The samples for microstructure analysis were sliced from the fractured surface including the exposed surface part (0–15 mm depth) after the strength test. The 0 mm depth represents the composites' surface in contact with

Table 1 Chemical composition of cement (by mass).

Material	CaO	SiO ₂	Al ₂ O ₃	Fe ₂ O ₃	SO ₃	MgO	Na ₂ O	K ₂ O	Ignition loss
Cement	65.61	17.66	4.74	4.00	3.05	1.31	0.16	1.00	2.13



the sulfate solution. The greater depth indicates a depth farther away from the exposed surface, namely deeper inside the composites.

Subsequently, the extracted samples were vacuum dried at 50 °C for 48 h, and then coated with gold, and finally examined by scanning electron microscopy (SEM, TESCAN VEGA 3 LMH with an acceleration voltage of 20 kV) assisted with energy dispersive spectroscopy (EDS).

X-ray diffraction (XRD, PANalytical Empyrean system using CuK α radiation, operating at 60 kV and 55 mA) was performed on powder samples from the extracted samples to identify the mineralogical composition within the composites.

3 Results and Discussion

3.1 Visual Inspection

Figure 2 shows the appearance of the composites after 12 months of partial exposure to sulfate attack. Cracks were observed along the edges of the immersed portions. The evaporation portions of all the composites were covered with a large number of white crystals (Fig. 2a). The XRD analysis (Fig. 3) indicates that the white products are thenardite (Na $_2$ SO $_4$). This was attributed to the fact that the sulfate solution entering the immersed portion (lower part) continued to migrate to the evaporation portion (upper part) under capillary suction, and then further penetrated to the composite surface with a lower relative humidity. As it approached the air, the sulfate solution became concentrated after water evaporation,

and thus Na $_2$ SO $_4$ crystallized on the outside of evaporation portion' surface. After wiping off the white crystals, different degrees of damage were observed for the composites (Fig. 2b). Among them, the evaporation portion of NC0 composite suffered serious surface scaling and flaking, and some cracks were also found along the edges. The damage degree of the composites decreased with the increase in nanosilica content. Nanosilica could react with Ca(OH) $_2$ to generate more C–S–H gels, thereby making the microstructure of the composites more compact, and their compactness increased with the increase of nanosilica content within a certain dosage range (Said et al. 2012; Yu et al. 2014; Sharma et al. 2019). The more compact microstructure of the nanosilica–cement composites limited the invasion and migration of sulfate ions, thereby relieving the damage caused by the sulfate attack.

3.2 Linear Expansion

Figure 4 displays the linear expansion of the composites partially exposed to sulfate attack. The linear expansion of all the composites increased gradually with time owing to the formation of expansive sulfate products. After 12 months, the linear expansion values of NC0, NC1, NC3 and NC5 composites were 2.49 mm/m, 1.72 mm/m, 0.79 mm/m and 0.28 mm/m, respectively. This indicated that adding nanosilica limited the expansion of the cement composites and their linear expansions reduced as the nanosilica content increased.

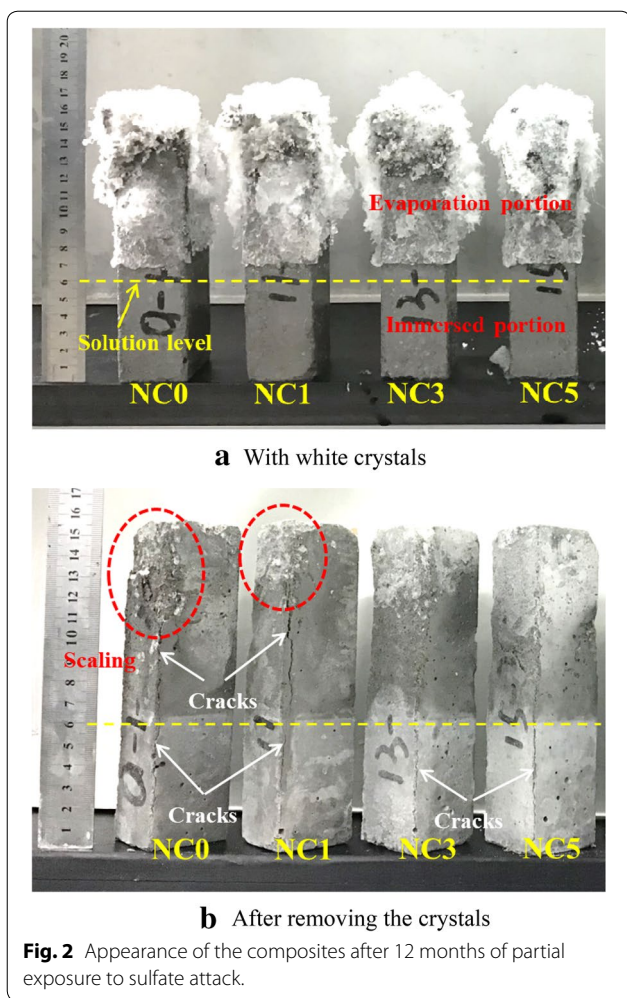


Fig. 2 Appearance of the composites after 12 months of partial exposure to sulfate attack.

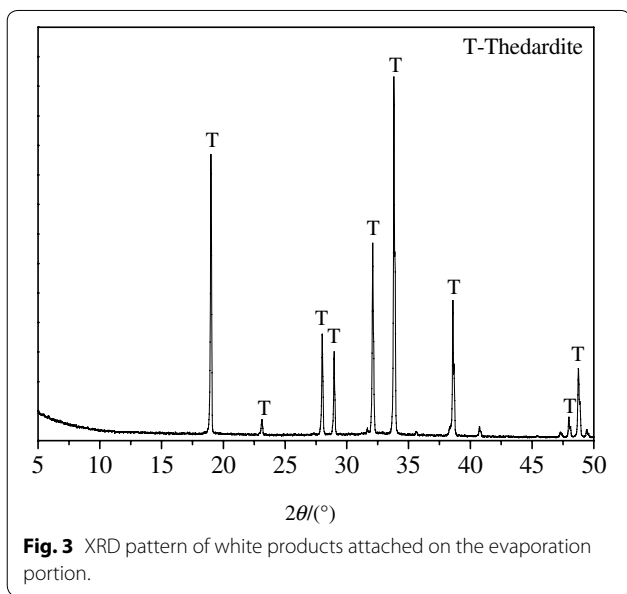


Fig. 3 XRD pattern of white products attached on the evaporation portion.

3.3 Compressive Strength Loss

Figure 5 shows the compressive strength loss of the composites after 12 months of partial exposure to sulfate attack. Both the immersed and evaporation portions of the composites suffered significant structural damage. The compressive strength loss of the immersed portion was lower than that of the evaporation portion for the composites blended with 0 to 3 wt% nanosilica, while this case was opposite for NC5 composite. In addition, the compressive strength loss of the composites decreased with the increase of nanosilica content. For instance, the compressive strength losses of the evaporation portions of NC0, NC1, NC3 and NC5 composites were 22.9%, 12.4%, 5.8% and 0.4%, respectively.

The above results indicated that the nanosilica–cement composites had better sulfate resistance compared to plain cement composites under partial exposure to sulfate attack, and their sulfate resistance increased as the nanosilica content increased (in the range of 0 to 5 wt% replacing cement by weight). Especially for NC5 composite, its damage degree was significantly low after 12 months of partial exposure to 5% Na₂SO₄ solution. This suggested that the nanosilica–cement composites could be applied in real partial exposure environments containing sulfate ions, where the sulfate concentration is much lower than the 5% used in this study.

3.4 SEM and EDS Analysis

Figure 6 illustrates the SEM pictures and EDS analysis of the immersed portion of the cement composite with 3% nanosilica (NC3) partially exposed to sulfate attack after 12 months. A large quantity of columnar crystals was found in the surface part of the immersed portion (Fig. 6a, b). According to the EDS analysis, the crystals mainly

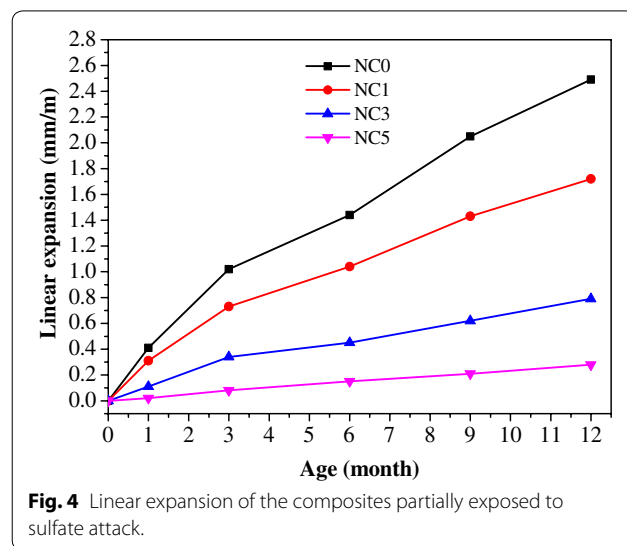
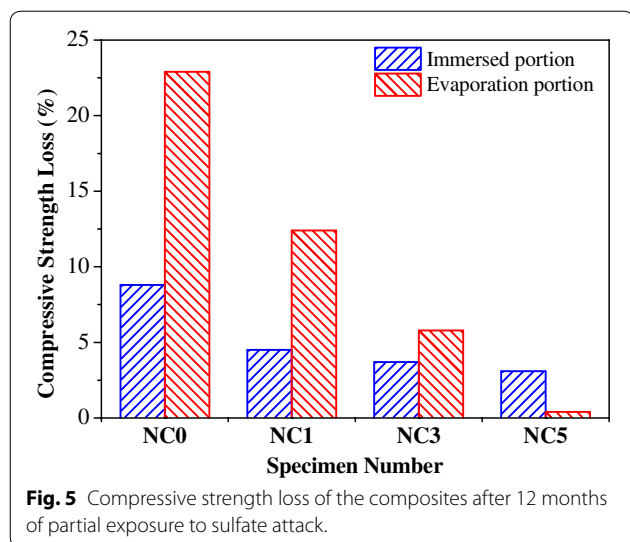
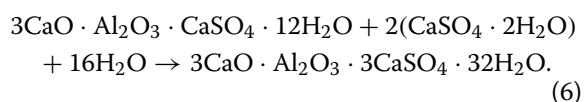
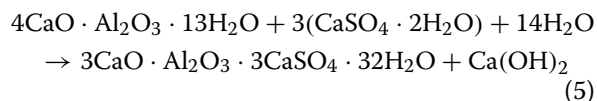
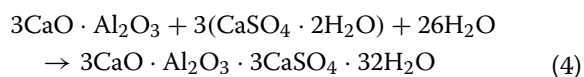
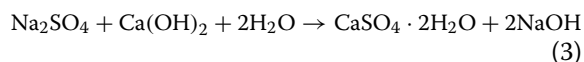


Fig. 4 Linear expansion of the composites partially exposed to sulfate attack.



contained Ca, S and O elements (Fig. 6d), indicating that this was gypsum. In the inner part (about 10–15 mm depth from the exposed surface), there were a great number of short needle-like crystals (Fig. 6c). The following elements were found in the crystals using EDS: Al, S, Ca and O (Fig. 6e), showing the formation of ettringite.

When Na₂SO₄ penetrated into the cement-based composites, it reacted with portlandite (Ca(OH)₂) to form gypsum (CaSO₄·2H₂O), which in turn could react with the alumina-bearing phases (e.g. 3CaO·Al₂O₃, 4CaO·Al₂O₃·13H₂O and 3CaO·Al₂O₃·CaSO₄·12H₂O) to form ettringite (3CaO·Al₂O₃·3CaSO₄·32H₂O), as follows (Tixier and Mobasher 2003):



The formation of sulfate products such as gypsum and ettringite could be expansive, resulting in the expansion, cracking, scaling and disintegration of cementitious composites. Meanwhile, the SEM/EDS results showed that the main sulfate products were gypsum and ettringite within the surface and inner parts, respectively in the immersed portion, which was consistent with the research conducted by Irassar et al.

(2003). This was attributed to the fact that the crystallization of gypsum occurred in a high sulfate concentration and ettringite was usually formed in a lower sulfate concentration (Lothenbach et al. 2010; Bellmann et al. 2006). Thus, gypsum was more likely to generate by crystallization within the surface part due to its higher sulfate concentration in this study. With the continuous migration of sulfate ions into the inside of the composites, the corresponding sulfate concentration gradually decreased, and then ettringite crystals were formed. The results showed that the immersed portion of the nanosilica–cement composite suffered chemical sulfate attack.

The SEM pictures and EDS analysis of the evaporation portion of NC3 composite partially exposed to sulfate attack after 12 months are shown in Fig. 7. The columnar crystals were also observed in the surface area of the evaporation portion (Fig. 7a, b). From the EDS results, these crystals were gypsum (Fig. 7d). Moreover, a large number of needle-like ettringite crystals were also formed in the inner part (Fig. 7c). In the evaporation portion, the Na₂SO₄ solution continued to migrate to the composite surface with a relative humidity less than 100%. After water evaporated from the surface area, the concentration of sulfate ions in the pore solution increased, leading to the formation of more gypsum in this area. Because the internal humidity of the evaporation portion was still high, the corresponding concentration of sulfate ions was lower, which resulted in ettringite becoming the main sulfate product in the inner area. The formation of gypsum and ettringite also resulted in cracking and scaling on the evaporation portion, as shown in Fig. 2b.

SEM pictures and EDS analysis of the immersed and evaporation portions of NC0 composite partially exposed to sulfate attack after 12 months are shown in Figs. 8 and 9, respectively. In consistency with NC3 composite, there was a large amount of gypsum crystals within the surface layer in both the immersed and evaporation portions of NC0 composite, and the sulfate products inside were mainly ettringite, indicating that the addition of nanosilica did not change the distribution characteristics of the sulfate products within the composites partially exposed to sulfate attack.

3.5 XRD Analysis

Subsequently, XRD analysis was performed to identify the presence of sulfate products within the composites containing different nanosilica content after partial exposure; the XRD results are shown in Fig. 10. Gypsum and ettringite were generated in both the immersed and evaporation portions of NC0 composite, and the peak intensities of the sulfate products in the evaporation portion

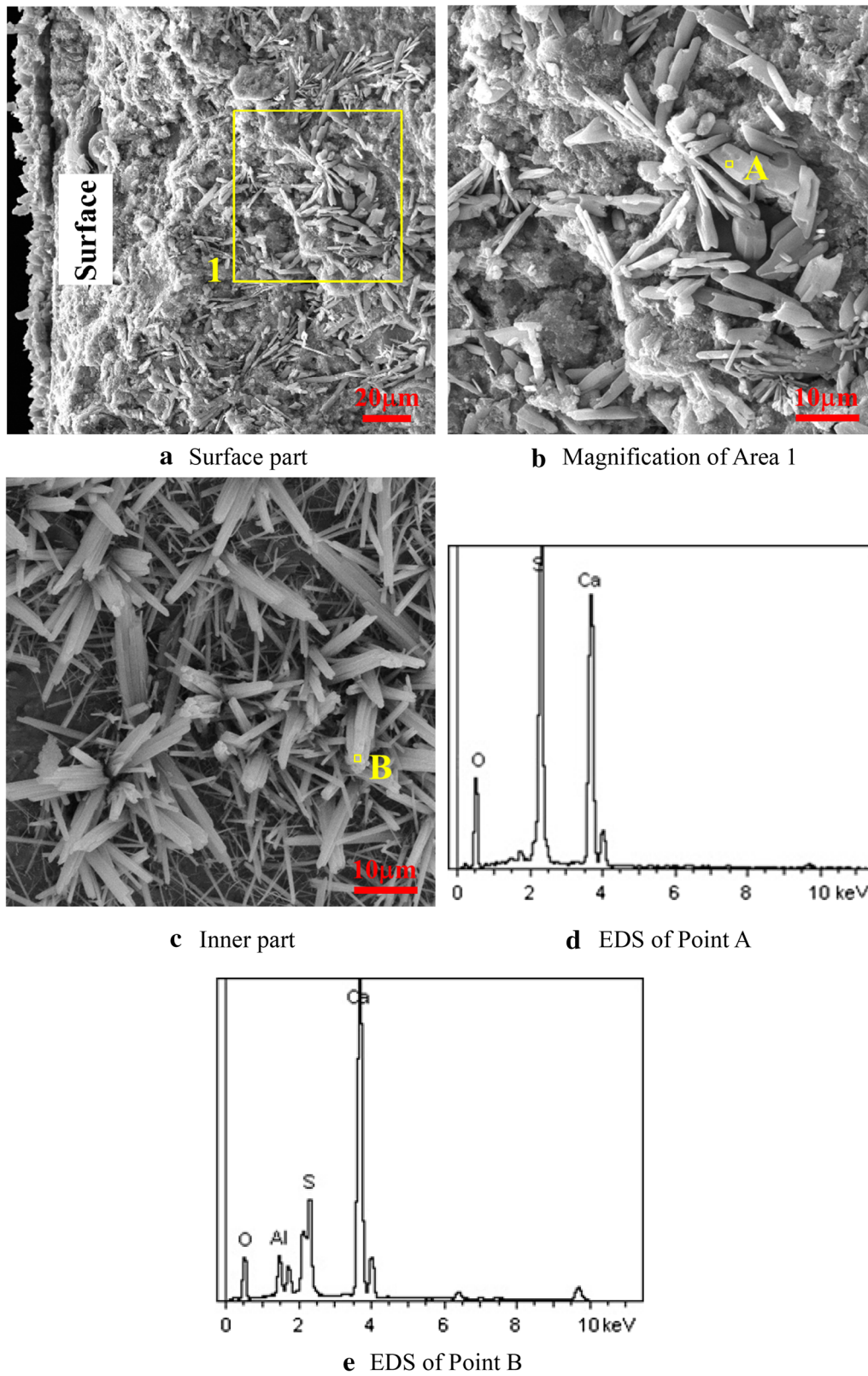


Fig. 6 SEM pictures and EDS analysis of the immersed portion of NC3 composite partially exposed to sulfate attack after 12 months.

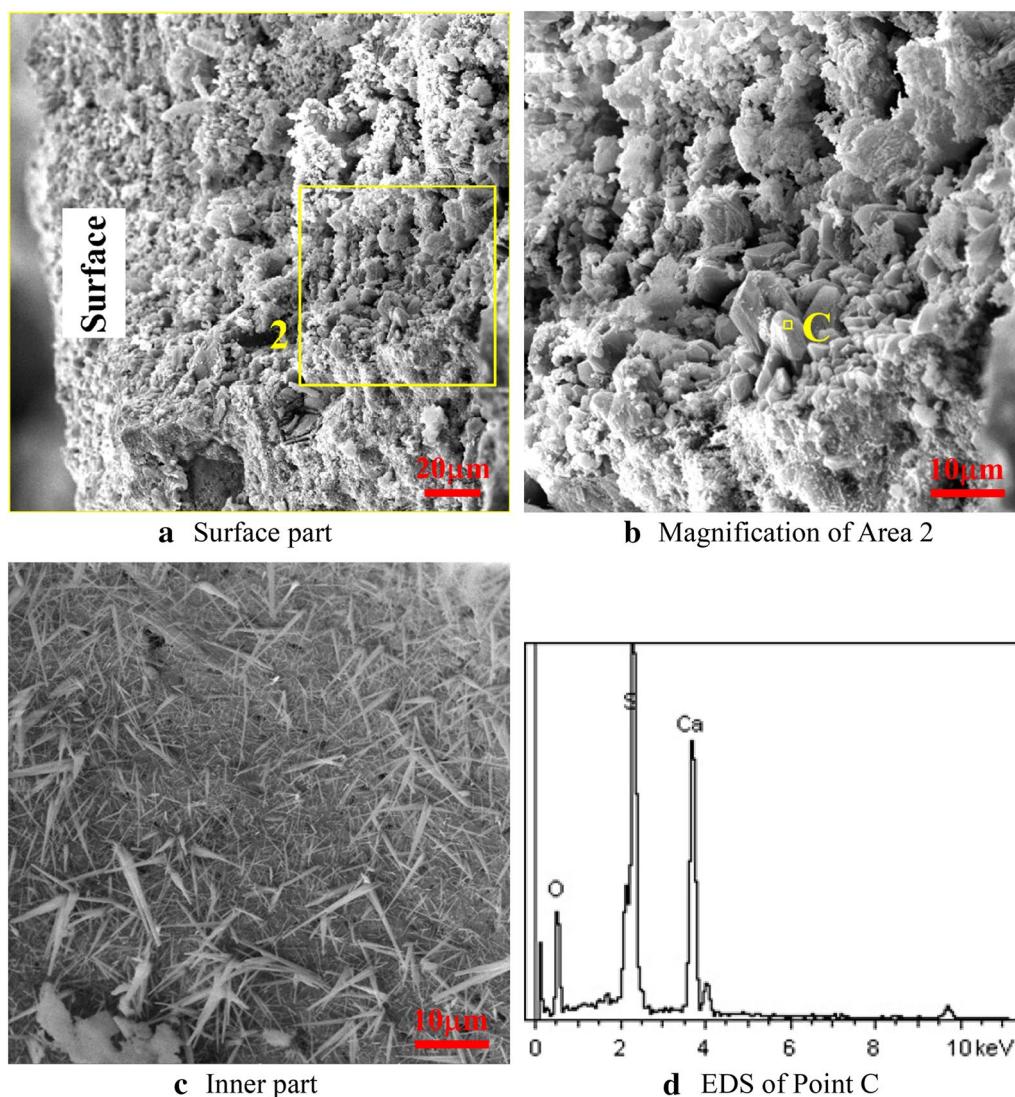


Fig. 7 SEM pictures and EDS analysis of the evaporation portion of NC3 composite partially exposed to sulfate attack after 12 months.

were greater than those in the immersed portion. This was caused by the relative humidity in the evaporation portion being lower than that in the immersed portion, and the corresponding pore solution having a higher concentration of ions. Thus, the saturation of gypsum and ettringite was attained faster, leading to the formation of more sulfate products, and consequently causing more severe damage for the evaporation portion compared with the immersed portion (Fig. 2b).

As previously mentioned, the more compact microstructure of the nanosilica–cement composites limited the invasion and migration of sulfate ions. Therefore, the incorporation of nanosilica reduced the amount of sulfate products in both the immersed and evaporation portions,

and their amount decreased with the increase of nanosilica content. Especially for NC5 composite, there was only a small amount of gypsum in the immersed portion, and the presence of gypsum and ettringite was hardly detected in the evaporation portion.

Besides, some calcite was found in the immersed portion of all the composites. This portion was fully immersed in the sulfate solution, isolating it from contact with CO₂ in the air, and as a result, carbonation would not occur. Therefore, the calcite mainly came from limestone powder in the cement. Meanwhile, the evaporation portion of all the composites also contained calcite, and its amount was not significantly different from that in the immersed portion, indicating a minimal degree of carbonation in

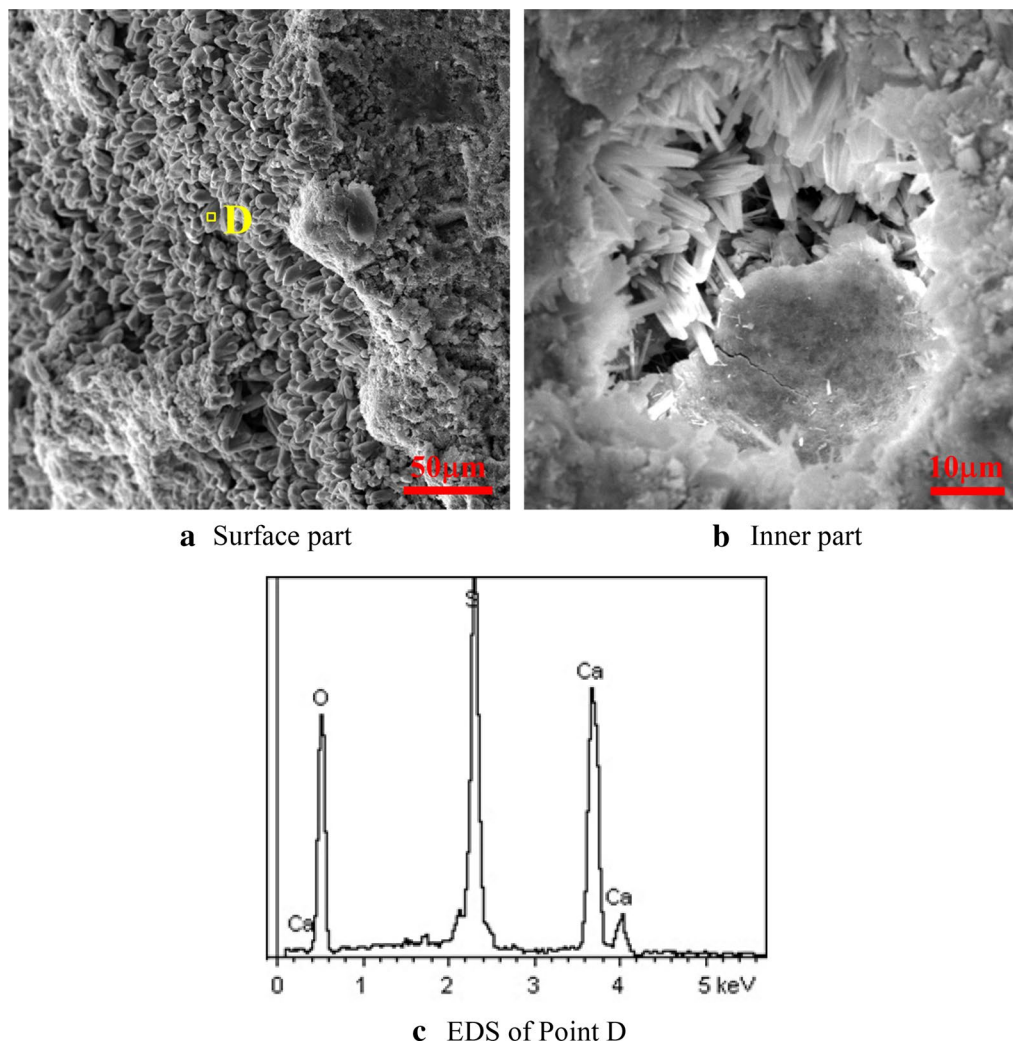


Fig. 8 SEM pictures and EDS analysis of the immersed portion of NCO composite partially exposed to sulfate attack after 12 months.

this portion. This was attributed to the attachment of the white crystals on the evaporation portion, which hindered the contact between composites and CO_2 .

Large amounts of thenardite crystals were formed on the outside of the evaporation portions' surface (Fig. 2a). This did not lead to the damage of the composites, only the crystallization of thenardite inside the composites would cause the destructive effect. However, no thenardite peak (at $2\theta = 28.03^\circ$, 32.12° , 33.83° and 38.61°) was identified within the evaporation portion of the composites through the XRD analysis. The results of Liu et al. (2011a, b, 2012) showed that the chemical sulfate attack was the main reason for the damage of the evaporation portion of non-carbonated cement-based composites; when the composites were completely carbonated, degradation was caused by sulfate salt crystallization. Na_2SO_4 did not crystallize in

cement-based composites probably because its crystallization needed to be carried out at a saturated concentration, while other less soluble salts, e.g. ettringite and gypsum, were preferably precipitated according to the chemical equilibrium theory below this concentration (Liu et al. 2011a). However, under an accelerated carbonation condition, portlandite in cement hydration products was most easily neutralized with CO_2 . As carbonation continued, other cement hydration products and unhydrated cement particles were converted into calcite, silica gel and aluminum gel, and these products would not react with sulfate. Thus, the chemical reaction between cementitious composites and Na_2SO_4 disappeared after the complete carbonation of the composites, which satisfied the condition of salt crystallization, hence Na_2SO_4 crystallized out (Liu et al. 2012). The XRD results displayed the minimal carbonation for

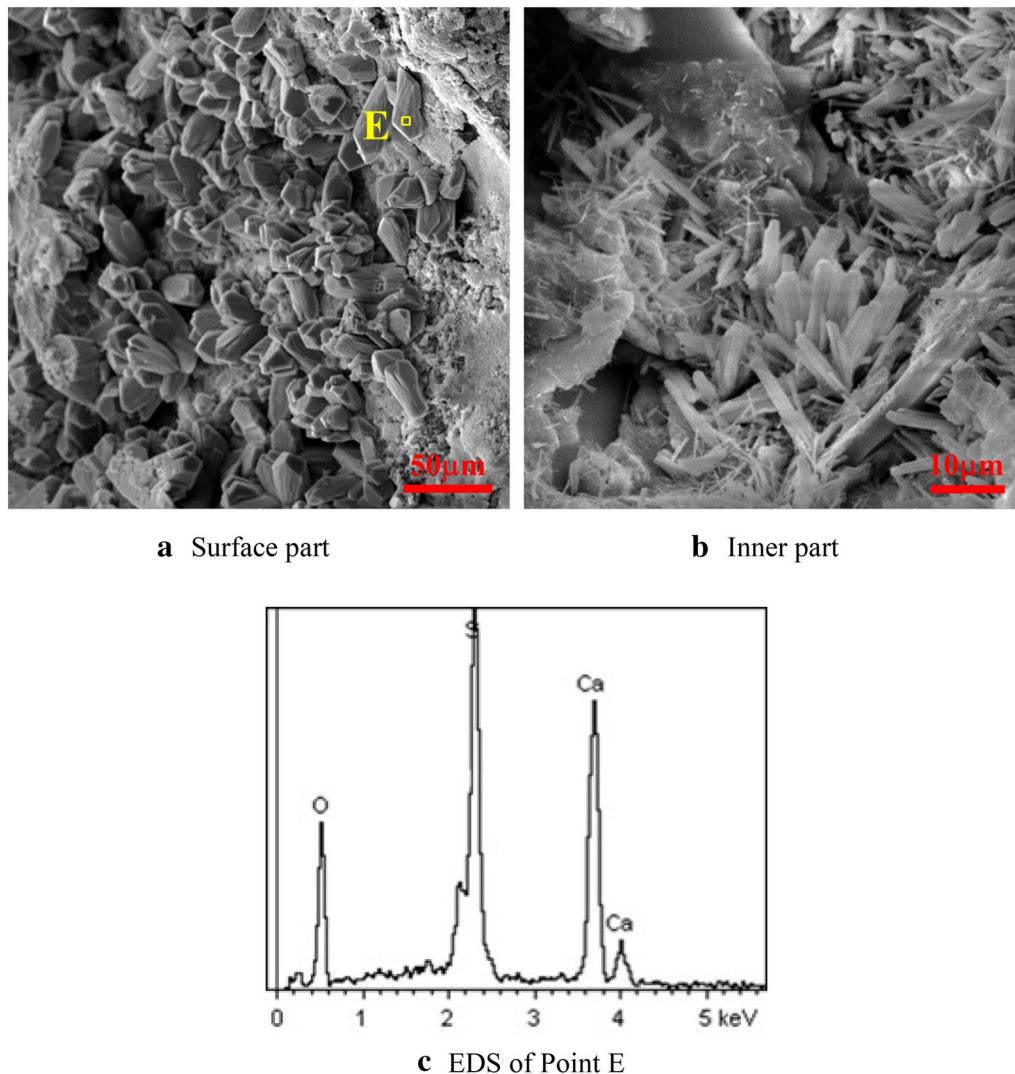


Fig. 9 SEM pictures and EDS analysis of the evaporation portion of NC0 composite partially exposed to sulfate attack after 12 months.

the evaporation portions of the cement composites in this study, which did not meet the conditions of salt crystallization. Meanwhile, large amounts of gypsum and ettringite crystals were generated in the evaporation portions, so it was concluded that the evaporation portions suffered chemical sulfate attack rather than sulfate salt crystallization according to the above viewpoint of Liu et al. (2011a, b, 2012).

4 Conclusions

Cement composites containing different nanosilica content were partially immersed in a 5% Na_2SO_4 solution under a room condition with 20 °C and 60% RH. The damage characteristic of the composites was investigated, and the microstructure change within them was analysed

using SEM, EDS and XRD. The conclusions of this study are as follows:

- 1 Nanosilica–cement composites had better sulfate resistance compared to plain cement composites under partial exposure to sulfate attack, and their sulfate resistance increased as the nanosilica content increased (in the range of 0 to 5 wt% replacing cement by weight).
- 2 The main sulfate products were gypsum and ettringite within the surface and inner parts, respectively in both the immersed and evaporation portions of the nanosilica–cement composites, which was consistent with the plain cement composite. Therefore, the incorporation of nanosilica did not change the distri-

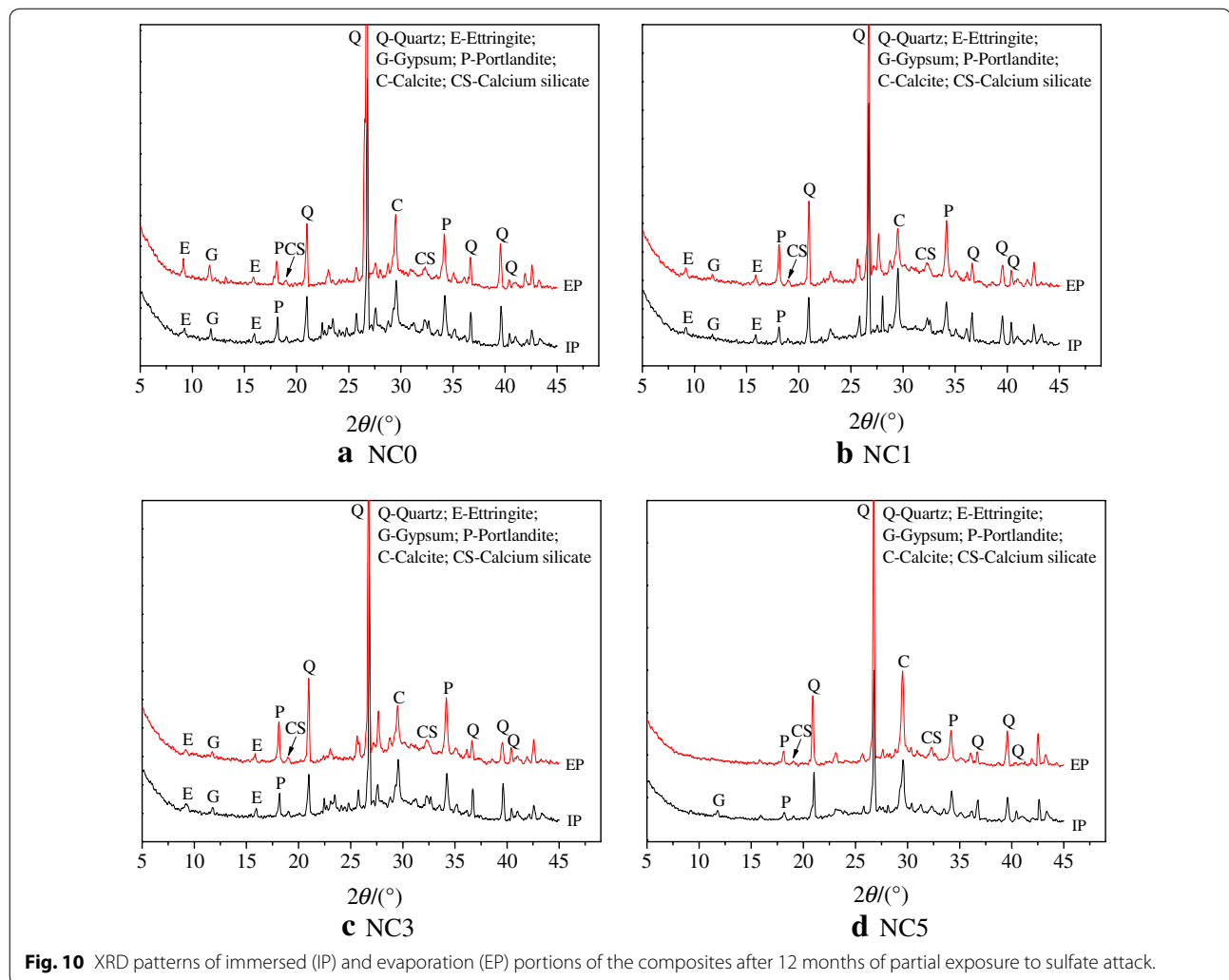


Fig. 10 XRD patterns of immersed (IP) and evaporation (EP) portions of the composites after 12 months of partial exposure to sulfate attack.

bution characteristics of the sulfate products within the composites partially exposed to sulfate attack. However, the addition of nanosilica reduced the amount of sulfate products in both the immersed and evaporation portions, and their amount decreased with the increase of nanosilica content.

- 3 The evaporation portions of the composites suffered chemical sulfate attack rather than sulfate salt crystallization.
- 4 Nanosilica–cement composites could be applied in real partial exposure environments containing sulfate ions. The durability of nanosilica–cement composites in a real sulfate environment would be investigated in following studies.

Acknowledgements

The authors acknowledge the financial support from the Natural Science Foundation of Chongqing from Chongqing Science and Technology Commission of China (No. cstc2019jcyj-msxmX0508 and No. cstc2016jcyjA0439), the Science and Technology Research Program of Chongqing Education

Commission of China (No. KJQN201801438) and the “Chunhui Plan” Cooperative Research Projects of Ministry of Education of China.

Authors' contributions

QH carried literature study and drafted the manuscript. QH and LZ carried out the experiment. CZ participated in the experiment studies. DL participated in discussing the results. CW provided some advices on the manuscript. All authors read and approved the final manuscript.

Funding

The costs of preparation of specimens and tests were paid by the following funding. Funder: Chongqing Science and Technology Commission of China. Award number: cstc2019jcyj-msxmX0508 and cstc2016jcyjA0439. Funder: Chongqing Education Commission of China. Award number: KJQN201801438. Funder: Ministry of Education of China.

Availability of data and materials

The datasets used and analysed during the current study are available from the corresponding author on reasonable request.

Competing interests

The authors declare that they have no competing interests.

Author details

¹ School of Civil and Architectural Engineering, Yangtze Normal University, Chongqing 408100, People's Republic of China. ² Green Intelligence

Environment School, Yangtze Normal University, Chongqing 408100, People's Republic of China. ³Chongqing Fuling Environment Protection Center for Shale Gas Technology & Development, Chongqing 480000, People's Republic of China.

Received: 17 May 2019 Accepted: 8 March 2020

Published online: 14 May 2020

References

- Atahan, H. N., & Dikme, D. (2011). Use of mineral admixtures for enhanced resistance against sulfate attack. *Construction Building Materials*, 25(8), 3450–3457.
- Atewi, Y. R., Hasan, M. F., & Güneyisi, E. (2019). Fracture and permeability properties of glass fiber reinforced self-compacting concrete with and without nanosilica. *Construction and Building Materials*, 226, 993–1005.
- Behfarnia, K., & Salemi, N. (2013). The effects of nano-silica and nano-alumina on frost resistance of normal concrete. *Construction and Building Materials*, 48, 580–584.
- Bellmann, F., Möser, B., & Stark, J. (2006). Influence of sulfate solutions concentration on the formation of gypsum in sulfate resistance test specimen. *Cement and Concrete Research*, 36(2), 358–363.
- Cho, Y. K., Jung, S. H., & Choi, Y. C. (2019). Effects of chemical composition of fly ash on compressive strength of fly ash cement mortar. *Construction and Building Materials*, 204, 255–264.
- Du, H., Du, S., & Liu, X. (2014). Durability performances of concrete with nano-silica. *Construction and Building Materials*, 73, 705–712.
- Eskander, S. B., Bayoumi, T. A., & Saleh, H. M. (2012). Performance of aged cement-polymer composite immobilizing borate waste simulates during flooding scenarios. *Journal of Nuclear Materials*, 420(1–3), 175–181.
- Ghazizadeh, S., Duffour, P., Skipper, N. T., & Bai, Y. (2018). Understanding the behaviour of graphene oxide in Portland cement paste. *Cement and Concrete Research*, 111, 169–182.
- Irassar, E. F., Bonavetti, V. L., & González, M. (2003). Microstructural study of sulfate attack on ordinary and limestone Portland cements at ambient temperature. *Cement and Concrete Research*, 33(1), 31–41.
- Jalal, M., Pouladkhanet, A., Harandi, O. F., & Jafari, D. (2015). Comparative study on effects of Class F fly ash, nano silica and silica fume on properties of high performance self-compacting concrete. *Construction and Building Materials*, 94, 90–104.
- Jo, B. W., Kim, C. H., & Lim, J. H. (2007). Investigations on the development of powder concrete with nano-SiO₂ particles. *KSCE Journal of Civil Engineering*, 11(1), 37–42.
- Liu, Z., Deng, D., De Schutter, G., & Yu, Z. (2011a). Micro-analysis of "salt weathering" on cement paste. *Cement & Concrete Composites*, 33(2), 179–191.
- Liu, Z., Deng, D., De Schutter, G., & Yu, Z. (2012). Chemical sulfate attack performance of partially exposed cement and cement + fly ash paste. *Construction and Building Materials*, 28(1), 230–237.
- Liu, Z., Hou, L., Deng, D., Zhang, F., & Hu, W. (2011b). Sodium sulfate salt crystallization distress on carbonated concrete. *Journal of the Chinese Ceramic Society*, 33(2), 179–191. (In Chinese).
- Liu, J., Yu, Q., Zuo, Z., Yang, F., Han, Z., & Qin, Q. (2019). Reactivity and performance of dry granulation blast furnace slag cement. *Cement & Concrete Composites*, 95, 19–24.
- Lothenbach, B., Bary, B., Le Bescop, P., Schmidt, T., & Leterrier, N. (2010). Sulfate ingress in Portland cement. *Cement and Concrete Research*, 40(8), 1211–1225.
- Mohseni, E., Miyandehi, B. M., Yang, J., & Yazdi, M. A. (2015). Single and combined effects of nano-SiO₂, nano-Al₂O₃ and nano-TiO₂ on the mechanical, rheological and durability properties of self-compacting mortar containing fly ash. *Construction and Building Materials*, 84, 331–340.
- Olsson, N., Nilsson, L., Åhs, M., & Baroghel-Bouny, V. (2018). Moisture transport and sorption in cement based materials containing slag or silica fume. *Cement and Concrete Research*, 106, 23–32.
- Said, A. M., Zeidan, M. S., Bassuoni, M. T., & Tian, Y. (2012). Properties of concrete incorporating nano-SiO₂. *Construction and Building Materials*, 36, 838–844.
- Saleh, H. M., El-Saied, F. A., Salah, T., & Hezo, A. A. (2019a). Influence of severe climatic variability on the structural, mechanical and chemical stability of cement kiln dust-slag-nanosilica composite used for radwaste solidification. *Construction and Building Materials*, 218, 556–567.
- Saleh, H. M., El-Saied, F. A., Salaheldin, T. A., & Hezo, A. A. (2018). Macro- and nanomaterials for improvement of mechanical and physical properties of cement kiln dust-based composite materials. *Journal of Cleaner Production*, 204, 532–541.
- Saleh, H. M., El-Sheikh, S. M., Elshereafy, E. E., & Essa, A. K. (2019b). Mechanical and physical characterization of cement reinforced by iron slag and titanate nanofibers to produce advanced containment for radioactive waste. *Construction and Building Materials*, 200, 135–145.
- Saleh, H. M., El-Sheikh, S. M., Elshereafy, E. E., & Essa, A. K. (2019c). Performance of cement-slag-titanate nanofibers composite immobilized radioactive waste solution through frost and flooding events. *Construction and Building Materials*, 223, 221–232.
- Saleh, H. M., & Eskander, S. B. (2019). Impact of water flooding on hard cement-recycled polystyrene composite immobilizing radioactive sulfate waste simulate. *Construction and Building Materials*, 222, 522–530.
- Sharma, U., Singh, L. P., Zhan, B., & Poon, C. S. (2019). Effect of particle size of nanosilica on microstructure of C-S-H and its impact on mechanical strength. *Cement & Concrete Composites*, 97, 312–321.
- Stefanidou, M., & Papayianni, I. (2012). Influence of nano-SiO₂ on the Portland cement pastes. *Composites Part B Engineering*, 43(6), 2706–2710.
- Tixier, R., & Mobasher, B. (2003). Modeling of damage in cement-based materials subjected to external sulfate attack. I: Formulation. *Journal of Materials in Civil Engineering*, 15(4), 305–313.
- Tobón, J. I., Payá, J., & Restrepo, O. J. (2015). Study of durability of Portland cement mortars blended with silica nanoparticles. *Construction and Building Materials*, 80, 92–97.
- Yu, R., Spiesz, P., & Brouwers, H. J. H. (2014). Effects of nano-silica on the hydration and microstructure development of Ultra-High Performance Concrete (UHPC) with a low binder amount. *Construction and Building Materials*, 65, 140–150.

Publisher's Note

Springer Nature remains neutral with regard to jurisdictional claims in published maps and institutional affiliations.

Submit your manuscript to a SpringerOpen® journal and benefit from:

- Convenient online submission
- Rigorous peer review
- Open access: articles freely available online
- High visibility within the field
- Retaining the copyright to your article

Submit your next manuscript at ► [springeropen.com](https://www.springeropen.com)